IMPLICIT SOLUTION OF UNCERTAIN VOLATILITY/TRANSACTION COST OPTION PRICING MODELS WITH DISCRETELY OBSERVED BARRIERS

P.A. FORSYTH* AND K.R. VETZAL†

Abstract. Option pricing models with uncertain volatility/transaction costs give rise to a nonlinear PDE. Previous work has focussed on explicit methods. However, pricing discretely observed barrier options requires a very small grid spacing near the barrier, and as a result, the maximum stable timestep for an explicit method is impractically small. A fully implicit method is developed for nonlinear option pricing models, and applied to arithmetic step options, where the option loses a fraction of its value for every day over the barrier.

Keywords: Option pricing, nonlinear, implicit
Running Title: Implicit uncertain volatility models
Acknowledgment: This work was supported by the National Sciences and Engineering Research Council of Canada, and Communications and Information Technology Ontario (CITO), funded by the Province of Ontario.
AMS Classification: 65N30
Last Revised: February 18, 1999

* Department of Computer Science, University of Waterloo, Waterloo, Ontario, Canada N2L 3G1, paforsyt@yoho.uwaterloo.ca

† Centre for Advanced Studies in Finance, University of Waterloo, kvetzal@watarts.uwaterloo.ca

1. Introduction. Options are extremely popular financial contracts for both individual and corporate investors. Option buyers are said to take long positions in the contracts, whereas option sellers take short positions. The two basic varieties of options are calls and puts. An investor who purchases a call option has the right to buy an underlying asset for a specified price (the strike price) on or before a specified expiry date. An investor who sells a call option collects the option price in exchange for taking on the obligation to deliver the underlying asset in return for the strike price if the option buyer exercises the option. A put option is similar except that the option buyer has the right to sell the underlying asset to the option seller for the strike price. Another basic distinction is between European and American style options. The former can be exercised only on the expiry date, while the latter may be exercised any time up to and including the expiry date. The value of an American option is thus constrained to be at least as high as its payoff from immediate exercise.

In addition to these standard types which are traded on many financial exchanges, there is a very large over-the-counter market in which financial institutions sell a variety of exotic options tailored to meet particular client demands. For example, Asian options feature payoffs which depend on the average price of the underlying asset during the contract. Lookback options depend on the highest or lowest price reached by the underlying asset. There is also a large number of different kinds of barrier options. In general, such contracts specify various payoffs if the underlying asset price reaches certain levels. For example, an up-and-out call option is like a standard call provided that the underlying asset price remains below a barrier level for the duration of the contract. Should the barrier level be reached, the contract is cancelled and the option's payoff is zero.

It is very important for financial institutions operating in the over-the-counter market to have accurate models in order to determine what price to charge for these individually-tailored contracts and how the hedge the risk exposure arising from their sale. The classic modelling approach [4, 19] assumes that the underlying asset's price moves over time according to geometric Brownian motion. By following a dynamic hedging strategy in which a portfolio containing the underlying asset and a risk free bond is continuously adjusted, it is possible to replicate the payoff of the option. This strategy turns out to be self-financing, i.e. the entire cost of executing it is incurred at the beginning as all subsequent transactions are financed through internally generated funds. The no-arbitrage principle then implies that the option price must equal the initial cost of constructing the replicating portfolio. This analysis leads to a linear second-order parabolic partial differential equation (PDE). Various different types of options may be valued by appropriate specification of boundary conditions. It is also important to note that strategies to hedge risks from selling options depend (in part) on the first and second derivatives of the option value with respect to the price of the underlying asset. As a result, it is essential to have accurate estimates of these derivatives for risk management purposes. For further details, the reader is referred to texts such as [12, 23].

The most fundamental input into an option pricing model is volatility, a measure of how much the underlying asset's price is likely to vary over time. Volatility estimation is by no means an exact science. Several approaches have been suggested, but none of them is completely satisfactory. Volatility estimators based on historical return data may not give accurate indications of future volatility, which is the object of interest for option valuation. Moreover, even though the standard industry pricing model [4] does not directly depend on the expected return of the underlying asset, estimates of the volatility parameter can be affected by the specification of the return [18]. In practice, it is more common to back out an estimate of volatility ("implied volatility") from observed prices of traded options. This also has drawbacks. Implied volatilities for the same stock differ across strike prices and maturity dates. It is not obvious how to derive a single volatility estimate from these various candidates. Moreover, it is not clear that this type of approach leads to reasonably good forecasts of future volatility [6]. Some authors have abandoned the idea of constructing a single volatility estimate from prices of traded options in favour of using a "volatility surface" (e.g. [21, 1]). This typically requires some interpolation and extrapolation of traded option data. Furthermore, some evidence indicates that it may not be any better than the single estimate approach in terms of predictive ability [9].

Recently, an alternative approach has been proposed in which it is assumed that the volatility is uncertain, but lies within a known range of values [2, 3, 23]. This setting differs fundamentally from that described above in that it is no longer the case that a unique option price is to be found. Instead a range of possible prices (from best case to worst case) is derived by solving a nonlinear PDE. This nonlinearity has an important practical consequence. A portfolio containing several options must be treated as a whole. Individual contracts cannot be handled separately and aggregated.

Traditionally, most option pricing models have ignored the effect of transaction costs. This is somewhat paradoxical, as there is no particular reason for options to exist in the absence of transaction costs (their payoff could always be attained by following the appropriate dynamic trading strategy). A couple of different approaches for handling transaction costs have been proposed. The simplest approach involves assuming that the replicating portfolio is adjusted at fixed points in time (e.g. [15, 5, 20]). More sophisticated models involve determining when to optimally adjust the replicating portfolio (e.g. [10, 8]). For present purposes, the simpler approach is of some interest because it leads to a nonlinear PDE of the same form as the uncertain volatility model.

Previously, explicit methods have been used to solve the nonlinear uncertain volatility/transaction cost PDE's [2, 3]. However, in the case of discretely observed barrier options, a very fine grid spacing is required near the barrier. Stability considerations may then require excessively small timesteps. The objective of this article is to develop an implicit method for solution of the nonlinear uncertain volatility pricing model. In particular, we apply the nonlinear PDE pricing model to the case of discretely observed arithmetic step options [16, 17]. These options lose a fraction of their value for every day that the price of the underlying asset is outside a barrier. Note that a conventional barrier option with immediate knockout is just a step option where the fraction of value lost is 100% the first time the price of the underlying asset is observed beyond a barrier.

2. Formulation. Following [2, 23], the best/worst case value $U(S,t)$ of an option with an uncertain volatility is given by

$$U_t + \frac{\sigma(\Gamma)^2}{2} S^2 U_{SS} + rSU_S - rU = 0 \tag{1}$$

where S is the underlying asset price, t is the time in the forward direction, and r is the risk free rate of return. If it is assumed that the volatility σ is such that

$$\sigma_{\min} \leq \sigma \leq \sigma_{\max} \tag{2}$$

but is otherwise uncertain, then the worst case value for an investor with a long position in the option is determined from the solution to equation (1) with $\sigma(\Gamma)$ given by:

$$\sigma(\Gamma)^2 \quad = \quad \begin{cases} \sigma_{\max}^2 & \text{if } \Gamma < 0 \\ \sigma_{\min}^2 & \text{if } \Gamma > 0 \end{cases} \tag{3}$$

where

$$\Gamma = U_{SS}. \tag{4}$$

Conversely, the best case value for an investor with a long position is determined from the solution to equation (1) with $\sigma(\Gamma)$ given by

$$\sigma(\Gamma)^2 \quad = \quad \begin{cases} \sigma_{\max}^2 & \text{if } \Gamma > 0 \\ \sigma_{\min}^2 & \text{if } \Gamma < 0 \end{cases} . \tag{5}$$

The worst case value for an investor with a short position (a negative payoff) in the option is given by the negative of the solution to equations (1) and (5). Consequently, the worst/best long case prices would correspond to the bid/ask prices for an option if the buyers/sellers priced the option assuming worst case scenarios.

The Leland [15] transaction cost model was extended for arbitrary payoffs in [11, 23]. In this case, the value of a long position is given by the solution to

$$U_t + \frac{\sigma_c^2}{2} S^2 \left[1 - \alpha \ \mathrm{sgn}(\Gamma)\right] U_{SS} + rSU_S - rU = 0 \tag{6}$$

and that of a short position is

$$U_t + \frac{\sigma_c^2}{2} S^2 \left[1 + \alpha \ \mathrm{sgn}(\Gamma)\right] U_{SS} + rSU_S - rU = 0 \tag{7}$$

where σ_c is the (known and constant) volatility. In [23], the transaction cost parameter α is given by

$$\alpha \quad = \quad \frac{\kappa}{\sigma_c} \sqrt{\frac{8}{\pi \delta t}} \tag{8}$$

where δt is the rehedging interval, and κS is the transaction cost per unit of the asset.

Equations (6-7) can be cast into the form of equation (1) if we define

$$\sigma(\Gamma)^2 = \begin{cases} \sigma_c^2[1 - \alpha \ \mathrm{sgn}(\Gamma)] & \text{for a long position} \\ \sigma_c^2[1 + \alpha \ \mathrm{sgn}(\Gamma)] & \text{for a short position} \end{cases} . \tag{9}$$

If we let

$$\begin{aligned} \sigma_{\min}^2 &= \sigma_c^2(1 - \alpha) \\ \sigma_{\max}^2 &= \sigma_c^2(1 + \alpha) \end{aligned} \tag{10}$$

then the transaction cost model becomes identical to an uncertain volatility model if

$$\begin{aligned} \sigma(\Gamma)^2 &= \left\{ \begin{array}{ll} \sigma_{\max}^2 & \text{if } \Gamma < 0 \\ \sigma_{\min}^2 & \text{if } \Gamma > 0 \end{array} \right\} \text{for a long position} \\ \sigma(\Gamma)^2 &= \left\{ \begin{array}{ll} \sigma_{\max}^2 & \text{if } \Gamma > 0 \\ \sigma_{\min}^2 & \text{if } \Gamma < 0 \end{array} \right\} \text{for a short position} \quad . \end{aligned} \tag{11}$$

Note that the transaction cost model becomes ill-posed, in general, if $\alpha > 1$ (since this causes a negative diffusion). In this case, an alternative model has been proposed which, in the case of a short position, uses $\sigma = \sigma_{\max}$ if $\Gamma > 0$, and $\sigma = 0$ if $\Gamma < 0$ with a suitable constraint [20]. In this work, we assume that $\alpha < 1$.

Consequently, the solution of equation (1) can be considered to be the value of best/worst case scenarios for an option with uncertain volatility, if $\sigma(\Gamma)$ is given from equations (3-5), or the value of long/short positions in an option with transaction costs given by the model in [11, 23], if $\sigma(\Gamma)$ is given from equation (9).

3. Step options. Recently, step options [16, 17] have been suggested as a way to alleviate some of the risk management problems associated with discrete barrier options. An option with an arithmetic step barrier loses a specified fraction of the payoff for every day the underlying asset is observed over a barrier. Alternatives to step options are delayed barrier and Parisian options [24, 7, 22]. In these contracts barrier events are triggered if the underlying asset remains outside a barrier level for a specified period of time. These types of delayed action barriers are cheaper than standard options, and provide inexpensive insurance if it is considered highly probable that the asset will not stay beyond a barrier for long periods of time. In the following, we will focus on simple arithmetic step barriers, although the numerical methods can be used without change for any combination of delayed, Parisian and step barriers. For ease of exposition, we consider an option with a single up-and-out knockout barrier. We will also assume that the barrier is discretely observed at daily intervals. It is a simple matter to extend these ideas to double barriers with different knock-out rates, knock-in barriers, and variable observation times.

We introduce a new state variable J, which is the cumulative number of observations of the asset price S which are not less than the barrier value S^*. The value of an option

U is then given as $U = U(S, J, t)$. Let t_i^+, t_i^- be the times just before and after the i^{th} observation time. Let J^* be the total number of observations such that if $J > J^*$, the option is worthless. Since $U(S, J > J^*, t) = 0$, we can restrict the computational values of J to be integers in the range $[0, J^*]$. The counter J is incremented as follows

$$J^+ = \begin{cases} \min(J^*, J^- + 1) & S \geq S^* \\ J^- & S < S^* \end{cases} . \tag{12}$$

No arbitrage considerations [23] then imply that

$$U(S, J^+, t^+) = U(S, J^-, t^-). \tag{13}$$

The payoff conditions at $t = T$ are then, for a linear step option,

$$U(S, J, t = T) \quad = \quad \begin{cases} (J^* - J)\max(S - K, 0) & \text{for a call} \\ (J^* - J)\max(K - S, 0) & \text{for a put} \end{cases} \tag{14}$$

where K is the exercise price.

4. Discretization. Away from observation dates t_i, we simply solve equation (1) backwards in time from $t = T$ to the present time $t = 0$, for each value of $J = 0, 1, \ldots, J^*$. Since there is no explicit J dependence away from observation dates, these equations for different values of J are completely independent. The terminal conditions for this set of one-dimensional equations is given by equation (14). At $S = 0$, no boundary condition is required since both the diffusion and drift terms vanish. At $S \to \infty$, at the expiry date of the option $t = T$, we impose a Dirichlet condition

$$U(S \to \infty, J, t = T) = \begin{cases} (J^* - J)S & \text{for a call} \\ 0 & \text{for a put} \end{cases} . \tag{15}$$

At observation dates, information is exchanged between the solutions for different values of J by applying the no-arbitrage condition (13). Equation (13) is also used to reset the Dirichlet conditions at $S \to \infty$ for each one-dimensional PDE problem. We assume that the discrete solution is known at $J = 0, 1, \ldots, J^*$, so that no interpolation is required in equation (13).

Equation (1) is discretized using a standard finite volume method. Equation (1) can be put into the more familiar form of the convection-diffusion equation if we define $\tau = T - t$

$$U_\tau = \frac{\sigma(\Gamma)^2}{2} S^2 U_{SS} + rSU_S - rU. \tag{16}$$

Consider the solution of equation (16) for a single value of J. To avoid notational clutter, we drop the dependence on J in the following. Let $U(S_i, \tau_n) = U_i^n$ be the discrete solution to equation (16) at asset value S_i, and time (going backwards) τ_n. Applying a standard finite volume method [26] then gives

$$\begin{aligned} A_i \left(\frac{U_i^{n+1} - U_i^n}{\Delta \tau} \right) \quad &= \quad (1 - \theta) \left(\sum_{j \in \eta_i} \gamma_{ij}^{n+1} (U_j^{n+1} - U_i^{n+1}) + \sum_{j \in \eta_i} \vec{L_{ij}} \cdot \mathbf{V}_i U_{ij+1/2}^{n+1} - A_i r U_i^{n+1} \right) \\ &+ \quad \theta \left(\sum_{j \in \eta_i} \gamma_{ij}^n (U_j^n - U_i^n) + \sum_{j \in \eta_i} \vec{L_{ij}} \cdot \mathbf{V}_i U_{ij+1/2}^n - A_i r U_i^n \right) \end{aligned} \tag{17}$$

where:

$$
\begin{aligned}
A_i &= (S_{i+1} - S_{i-1})/2 \\
\eta_i &= \{i-1, i+1\} \\
\Delta\tau &= \tau^{n+1} - \tau^n \\
\theta &= \text{timeweighting parameter} \\
\gamma_{ij}^n &= \frac{\sigma(\Gamma_i^n)^2 S_i^2}{2|S_j - S_i|} \\
U_{ij+1/2}^{n+1} &= \text{value of } U \text{ at the face between} \\
&\quad\ \text{node } i \text{ and node } j. \\
\mathbf{V}_i &= (-rS_i)\hat{\mathbf{i}} \\
\vec{L}_{ij} &= \begin{cases} -\hat{\mathbf{i}} & \text{if } j = i+1 \\ +\hat{\mathbf{i}} & \text{if } j = i-1 \end{cases} \\
\hat{\mathbf{i}} &= \text{unit vector in the positive S direction.}
\end{aligned} \tag{18}
$$

The usual finite difference approximation is used for Γ_i^n

$$
\Gamma_i^n = \frac{\left(\dfrac{U_{i+1}^n - U_i^n}{S_{i+1} - S_i}\right) - \left(\dfrac{U_i^n - U_{i-1}^n}{S_i - S_{i-1}}\right)}{(S_{i+1} - S_{i-1})/2}. \tag{19}
$$

An automatic timestep selector [14] was used with either fully implicit ($\theta = 0$) or Crank-Nicolson ($\theta = 1/2$) timeweighting.

The face value $U_{ij+1/2}^{n+1}$ is evaluated using either central weighting or a flux limiter [27], to ensure non-oscillatory solutions

$$
U_{ij+1/2}^{n+1} = \begin{cases} (U_i^{n+1} + U_j^{n+1})/2 & \text{if } \gamma_{ij}^{n+1} + \vec{L}_{ij} \cdot \mathbf{V}_i/2 > 0 \\ \text{second order flux limiter[27]} & \text{otherwise} \end{cases}. \tag{20}
$$

For ease of exposition, suppose that

$$
\gamma_{ij}^{n+1} + \vec{L}_{ij} \cdot \mathbf{V}_i/2 \geq 0 \ ; \ \forall i, j \tag{21}
$$

and that fully implicit time weighting is used in equation (17). Then, we can write equation (17) as

$$
\begin{aligned}
A_i\left(\frac{U_i^{n+1} - U_i^n}{\Delta\tau}\right) &= \sum_{j\in\eta_i} \gamma_{ij}^{n+1}(U_j^{n+1} - U_i^{n+1}) + \sum_{j\in\eta_i} \vec{L}_{ij} \cdot \mathbf{V}_i \frac{(U_i^{n+1} + U_j^{n+1})}{2} - A_i r U_i^{n+1} \\
&= \sum_{j\in\eta_i} \left(\gamma_{ij}^{n+1}(U_j^{n+1} - U_i^{n+1}) + \frac{\vec{L}_{ij} \cdot \mathbf{V}_i}{2} U_j^{n+1}\right) \\
&+ U_i^{n+1} \sum_{j\in\eta_i} \frac{\vec{L}_{ij} \cdot \mathbf{V}_i}{2} - A_i r U_i^{n+1}.
\end{aligned} \tag{22}
$$

Noting that

$$\sum_{j \in \eta_i} \vec{L_{ij}} \cdot \mathbf{V}_i = 0 \tag{23}$$

at all interior points, equation (22) becomes

$$\begin{aligned} A_i \left(\frac{U_i^{n+1} - U_i^n}{\Delta\tau} \right) &= \sum_{j \in \eta_i} \left(\gamma_{ij}^{n+1} (U_j^{n+1} - U_i^{n+1}) + \frac{\vec{L_{ij}} \cdot \mathbf{V}_i}{2} U_j^{n+1} \right) \\ &- U_i^{n+1} \sum_{j \in \eta_i} \frac{\vec{L_{ij}} \cdot \mathbf{V}_i}{2} - A_i r U_i^{n+1} \\ &= \sum_{j \in \eta_i} \left(\gamma_{ij}^{n+1} + \frac{\vec{L_{ij}} \cdot \mathbf{V}_i}{2} \right) (U_j^{n+1} - U_i^{n+1}) - A_i r U_i^{n+1}. \end{aligned} \tag{24}$$

Let

$$U_i^n = \frac{W_i^n}{(1 + r\Delta\tau)^n} \tag{25}$$

and substituting for U_i^n in equation (24) using equation (25) gives

$$A_i \left(\frac{W_i^{n+1} - W_i^n}{\Delta\tau} \right) = \sum_{j \in \eta_i} \left(\gamma_{ij}^{n+1} + \frac{\vec{L_{ij}} \cdot \mathbf{V}_i}{2} \right) \frac{(W_j^{n+1} - W_i^{n+1})}{(1 + r\Delta\tau)} \tag{26}$$

which implies that (noting equation (21))

$$\begin{aligned} W_i^{n+1} \geq W_j^{n+1} \ ; \ j \in \eta_i \ &\Rightarrow \ W_i^{n+1} - W_i^n \leq 0 \\ W_i^{n+1} \leq W_j^{n+1} \ ; \ j \in \eta_i \ &\Rightarrow \ W_i^{n+1} - W_i^n \geq 0 \end{aligned} \tag{27}$$

and therefore solutions to equation (26) are local extremum diminishing (LED) [13]. Since $U_i^n = W_i^n/(1 + r\Delta\tau)^n$, it follows that

$$\begin{aligned} U_i^{n+1} \geq U_j^{n+1} \ ; \ j \in \eta_i \ &\Rightarrow \ U_i^{n+1} - \frac{U_i^n}{1 + r\Delta\tau} \leq 0 \\ U_i^{n+1} \leq U_j^{n+1} \ ; \ j \in \eta_i \ &\Rightarrow \ U_i^{n+1} - \frac{U_i^n}{1 + r\Delta\tau} \geq 0 \end{aligned} \tag{28}$$

which implies that the solutions to equation (17) have a *discounted* LED property (i.e. local extrema are diminished relative to the discounted future value, where it should be recalled that $\tau_n \to \tau_{n+1}$ is moving backwards in time). In general, an LED method ensures that spurious oscillations will not be generated in the solution.

This holds for any timestep and any grid size, and regardless of the fact that γ_{ij}^n is a function of $\Gamma = (U_{SS})_i^n$. The condition (21) is satisfied at most nodes (for typical values of r, σ) if the underling process is simple geometric Brownian motion except possibly as $S_i \to 0$ [27]. For problems where the asset follows an alternative stochastic process (e.g. interest rate models), condition (21) may be violated at many nodes. In this case, the techniques in [25] can be used to show that equation (17) will be non-oscillatory if a flux-limiter is used instead of central weighting. In this work, we use the face values $U^{n+1}_{ij+1/2}$ given by equation (20), which ensures that the solution is *discounted* LED regardless of timestep size (for a fully implicit method) and for more complex forms for the underlying stochastic process. Note that if we had started with a conservative form for the first order term in equation (16), i.e.

$$U_\tau = \frac{\sigma(\Gamma)^2}{2} S^2 U_{SS} + (rSU)_S - 2rU. \tag{29}$$

then the above LED property would not hold in general.

5. Solution of nonlinear equations. The discrete equations (17) are non-linear due to the $\sigma(\Gamma)^2$ term in equation (1). This is actually a fairly mild non-linearity. To see this, suppose that an uncertain volatility model with equation (5) is specified. The nonlinear term in equation (17) then has the form

$$\begin{array}{ll} \sigma^2_{\max}\Gamma^{n+1}_i & \text{if } \Gamma^{n+1}_i > 0 \\ \sigma^2_{\min}\Gamma^{n+1}_i & \text{if } \Gamma^{n+1}_i < 0 \end{array} \tag{30}$$

which is a continuous function of Γ^{n+1}_i, and has well defined derivatives with respect to Γ^{n+1}_i everywhere but at $\Gamma^{n+1}_i = 0$. In the following, a Newton iteration will be used to solve the nonlinear algebraic equations. Consequently, a straightforward method for handling the problem at $\Gamma = 0$ is to simply use the limiting derivative value in the Jacobian as $\Gamma \to 0$ from the left or right. We will refer to this approach in the following as Newton iteration with no smoothing.

Another possibility for alleviating the difficulty near $\Gamma = 0$ would be to smooth the nonlinearity by redefining $\sigma(\Gamma)^2$. For example, we could replace equation (3) by

$$\sigma(\Gamma)^2 = \frac{\exp(-\beta\Gamma)\sigma^2_{\max} + \exp(\beta\Gamma)\sigma^2_{\min}}{\exp(-\beta\Gamma) + \exp(\beta\Gamma)} \; . \tag{31}$$

For large β, this is a good approximation to equation (3). In the following, we will refer to the use of equation (31) as Newton iteration with smoothing.

The Newton iteration for a given timestep is deemed to have converged when

$$\max_i \frac{|(U^{n+1}_i)^{k+1} - (U^{n+1}_i)^k|}{\max(|(U^{n+1}_i)^{k+1}|, |(U^n_i)|, 1.0)} < tol \tag{32}$$

where $(U^{n+1}_i)^k$ is the k^{th} iterate for U^{n+1}_i.

6. Uncertain volatility option. We first consider an arithmetic linear step knockout option priced with an uncertain volatility model. In this and all subsequent examples, we assume daily barrier observation. Data for these problems is given in Table 1.

Table 2 demonstrates the convergence of the PDE method as the the grid size and timestep size is reduced. It was found that the uncertain volatility model was very

TABLE 1
Data for uncertain volatility option.

σ	$.25 - .50$
	$.15 - .30$
r	.05
Time to expiry	.5 years
Exercise price (K)	\$100
Barrier location	\$120
Barrier type	arithmetic step [17], observed daily
Time to full knockout	1, 5, 10, 20 days

sensitive to the grid spacing near the barrier, much more so than a similar problem with a constant volatility. This is undoubtedly because the barrier causes a rapid change in the solution, which is amplified by the computation of Γ_i^{n+1} (equation (19)).

The finest grid (401 nodes) used a spacing of $\Delta S_i \simeq 6\times 10^{-4}$ near the barrier, which, from Table 2, is sufficient for penny accuracy. Consequently, all examples reported in the following used this grid with 401 nodes. The solution was also sensitive to the initial timestep size after barrier observation. The runs shown in Table 2 used a timestep of 1×10^{-5} after each observation (on the finest grid). An error controlled timestep selector [14] then increased the timestep until the next observation.

Note that the maximum stable explicit timestep would be about

$$\frac{\Delta\tau S_i^2 \sigma(\Gamma)^2}{2\Delta S_i^2} \simeq \frac{1}{2}. \tag{33}$$

The worst case for equation (33) is near the barrier, with $S_i = 120$, $\Delta S_i = 6 \times 10^{-4}$, and $\sigma = .5$, which gives

$$\Delta\tau_{\max} \simeq 10^{-10}. \tag{34}$$

It is well known that a Crank-Nicolson method may generate spurious oscillations unless the timestep is of the order of the explicit timestep [28]. Our attempts to use Crank-Nicolson timestepping required a very large number of nonlinear iterations. Since the timestep selector cut the timestep if the nonlinear iteration did not converge to within the specified tolerance (equation (32)) after ten iterations, the successful timestep sizes became impractically small. A close examination of the computed solution revealed that small oscillations generated by the Crank-Nicolson method (for $\Delta\tau > \Delta\tau_{\max}$) caused the computed estimate of Γ_i^{n+1} to change sign each iteration, so that convergence could not be obtained. However, Crank-Nicolson timestepping on a similar problem with a constant volatility produced reasonable solutions with much larger timesteps, indicating that the nonlinear term amplified oscillations. Consequently, fully implicit timestepping is used in all the following computations. (Recall that fully implicit methods are guaranteed to be *discounted* LED for the nonlinear discrete equation (17) for any timestep

TABLE 2

Convergence of option values, step barrier (linear knockout, time to full knockout $1, 5, 10, 20$ *days), barrier at \$120, barrier observed daily, call option,* $T = .5$, $r = .05$. *Range of* $\sigma = .25 - .50$. *Fully implicit timestepping with automatic timestep selector [14]. The finer grids used smaller timestep control parameters.*

Time to full knockout	Nodes	Option Value (S =\$100)	Option Value (S =\$120)
Best Case			
1 day	201	3.2381	0.5875
	401	3.2325	0.5925
5 days	201	3.8532	1.1286
	401	3.8535	1.1349
10 days	201	4.3598	1.6393
	401	4.3624	1.6460
20 days	201	5.1153	2.4837
	401	5.1194	2.4891

size). Figure 1 gives a graphical comparison of the hedging parameters gamma (U_{SS}) and delta (U_S) for the coarse and fine grid computations.

The computed gamma, for the uncertain volatility computations, was very sensitive to the Newton iteration convergence tolerance (32). Figure 2 shows that the computed values of gamma (U_{SS}) near the barrier are very poor unless $tol \simeq 10^{-6}$. Consequently, this value of the tolerance was used in all the examples reported in this work.

The effect of using the smoothing approximation (31) near $\Gamma = 0$ compared with no smoothing is shown in Table 3. Note that the total timesteps and nonlinear iterations are given for all $J^* + 1 = 11$ one-dimensional problems. Rather surprisingly, use of the smoothed iteration was actually worse, in terms of total nonlinear iterations, compared to the non-smoothed algorithm. A similar result was obtained in [26] when using a penalty method to enforce the American option constraint. As a result, we will use the non-smoothed method for all computations in this paper.

The average timestep size for the the runs with no smoothing was about $\simeq .5/800 = 6 \times 10^{-4}$). This compares with a maximum timestep of about 10^{-10} for an explicit timestep (equation (34)). Although increasing the timestep control parameters resulted in larger average timesteps, the total number of nonlinear iterations decreased only slightly.

Figure 3 shows two scenarios, volatility in the ranges $.25 - .50$ and $.15 - .30$, for an arithmetic step barrier with ten days to full knockout, as well as the prices for constant volatilities. Note that the best and worst case prices are outside the envelopes of prices for constant volatilities. This because $\Gamma = U_{SS}$ has both positive and negative values for barrier options (see equation 3)).

Figure 4 shows the effect of varying the time to complete knockout for best case option values, delta, and gamma. Similar results are given for the worst case prices, delta and gamma in Figure 5. We also give the results for the limiting case of a single

FIG. 1. *Convergence of option delta (U_S) and gamma (U_{SS}). Step barrier (linear knockout, time to full knockout* 5 *days), barrier at \$120, barrier observed daily, call option, $T = .5$, $r = .05$. Best case long price for range of $\sigma = .25 - .50$ (negative of worst case for short position). Coarse grid has* 201 *nodes in the S direction, fine grid has* 401 *nodes. The finer grid uses smaller timesteps.*

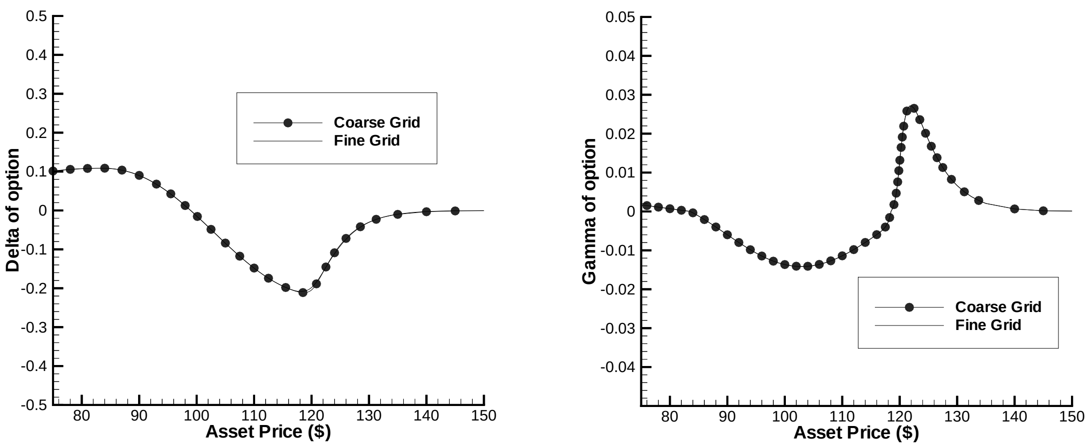

TABLE 3

Effect of smoothing parameter on the convergence of the nonlinear iteration. Best case, step barrier (linear knockout, time to full knockout 10 *days), barrier at \$120, barrier observed daily, call option, $T = .5$, $r = .05$. Range of $\sigma = .25 - .50$. Fully implicit timestepping with automatic timestep selector [14]. Total timesteps and nonlinear iterations reported for total of $J^* + 1 = 11$ one-dimensional PDE problems.*

Smoothing parameter β	Option Value ($S =$\$100)	Option Value ($S =$\$120)	Total nonlinear iterations	Total timesteps
No Smoothing	1.6460	4.3624	29295	8741
10^5	1.6461	4.3624	59573	11712
10^4	1.6458	4.3624	76125	13121
10^3	1.6437	4.3599	62009	10762
10^2	***	***	***	***

*** *failed to complete in maximum timesteps*

FIG. 2. *Effect of nonlinear convergence tolerance on option gamma. Step barrier (linear knockout, time to full knockout* 10 *days), barrier at \$120, barrier observed daily, call option,* $T = .5$, $r = .05$. *Best case long price for range of* $\sigma = .25 - .50$ *(negative of worst case for short position). Fine grid (*401*) nodes.*

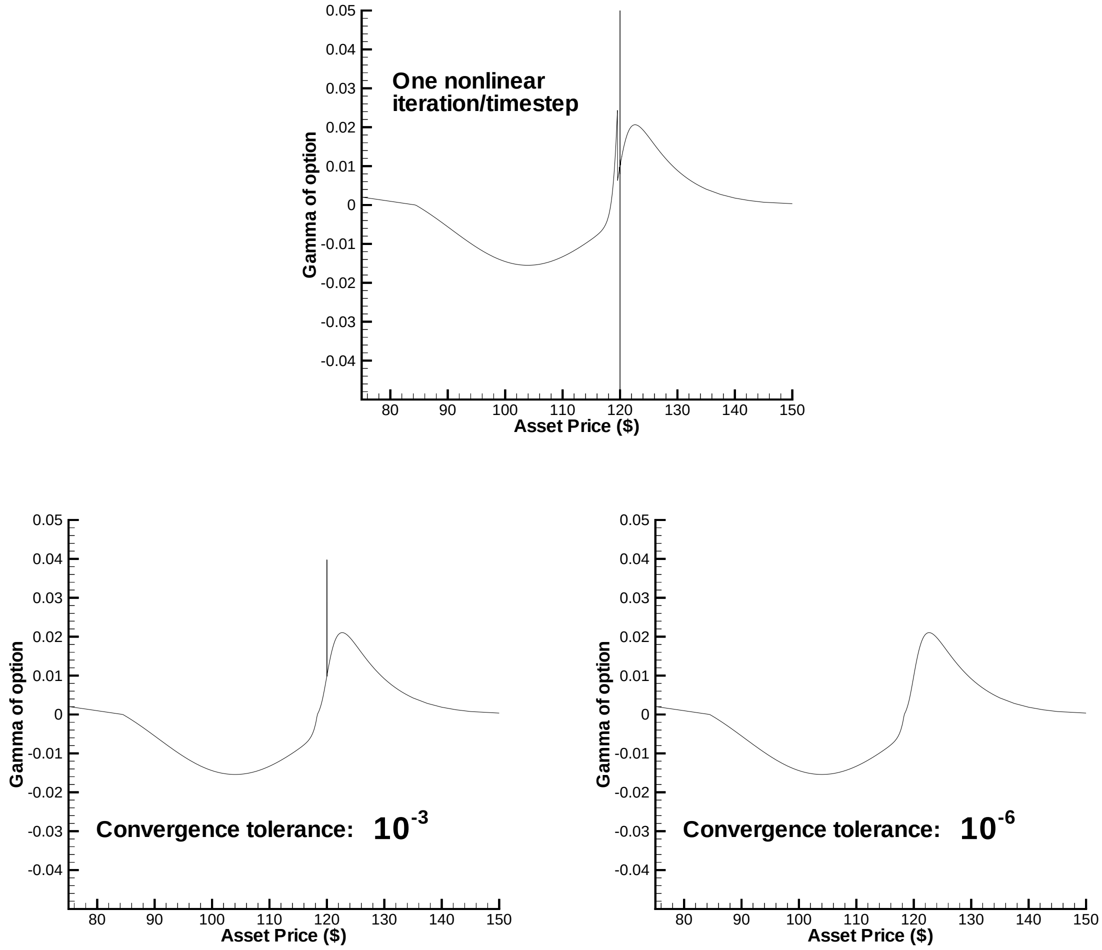

FIG. 3. *Option Value. Step barrier (linear knockout, time to full knockout* 10 *days), barrier at \$120, barrier observed daily, call option,* $T = .5$, $r = .05$. *Left: best case and worst cases (range of* $\sigma = .25 - .50$*), and constant* $\sigma = .25, .5$ *shown; right: best case and worst cases (range of* $\sigma = .15 - .30$*), and constant* $\sigma = .15, .30$ *shown.*

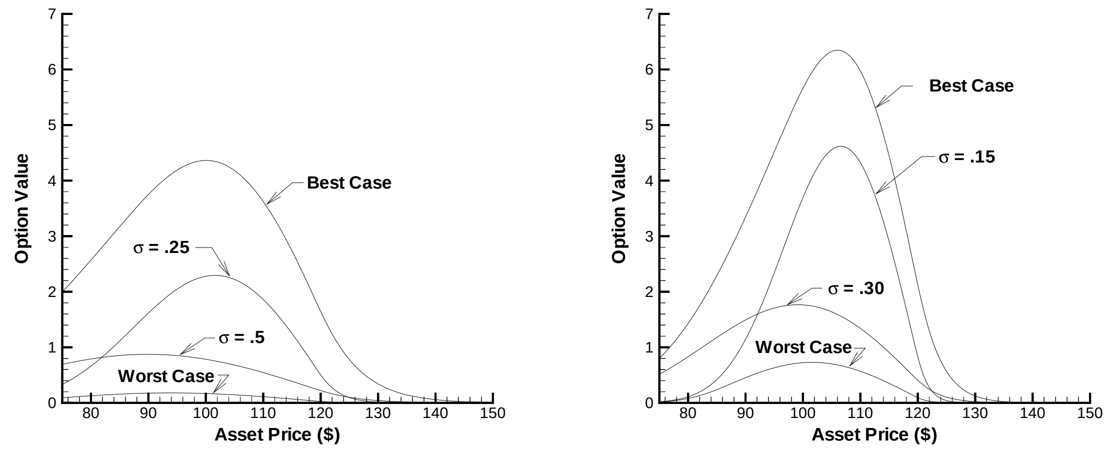

day to full knockout, which is a standard knockout barrier contract.

7. Option prices with transaction costs. Figure 6 shows the option prices for a linear step barrier option with 5, 10, 20 days to full knockout, priced using the transaction cost model. The data for these examples is given in Table 4. With a transaction cost parameter of $\beta = .25$ and volatility $\sigma = .40$, this corresponds to an uncertain volatility model (equation (10)) with

$$\begin{aligned} \sigma_{\max} &= 0.4472 \\ \sigma_{\min} &= 0.3464 \end{aligned} \tag{35}$$

For at-the-money options, the transaction cost models indicate that short prices are more than double long prices. This is not surprising, since it is well known that dynamically hedging a barrier option is very expensive. For barrier options, it is more common to use a static hedging strategy [23].

8. Conclusions. Use of an uncertain volatility/transaction cost model gives rise to a nonlinear PDE. If small grid spacing is necessary, near a discretely observed barrier for example, then an implicit method is required. The nonlinear uncertain volatility/transaction cost model, applied to arithmetic step options, is very sensitive to the grid spacing near the barrier and the Newton iteration convergence tolerance.

Only a fully implicit timestepping method was feasible for these problems. Small oscillations generated by a Crank-Nicolson method caused failure of the nonlinear iteration except for impractically small timesteps (of the order of the explicit timestep size). The fully implicit discretization used in this work, coupled with an appropriate discretization of the first order term, is guaranteed to have a *discounted* LED property, for any timestep size, which ensures that spurious oscillations will not cause problems in computing the nonlinear terms in the discrete equations.

FIG. 4. *Best case option value, delta (U_S), and gamma (U_{SS}). Step barrier (linear knockout, time to full knockout* $1, 5, 10, 20$ *days), barrier at \$120, barrier observed daily, call,* $T = .5$, $r = .05$, *range of* $\sigma = .25 - .50$.

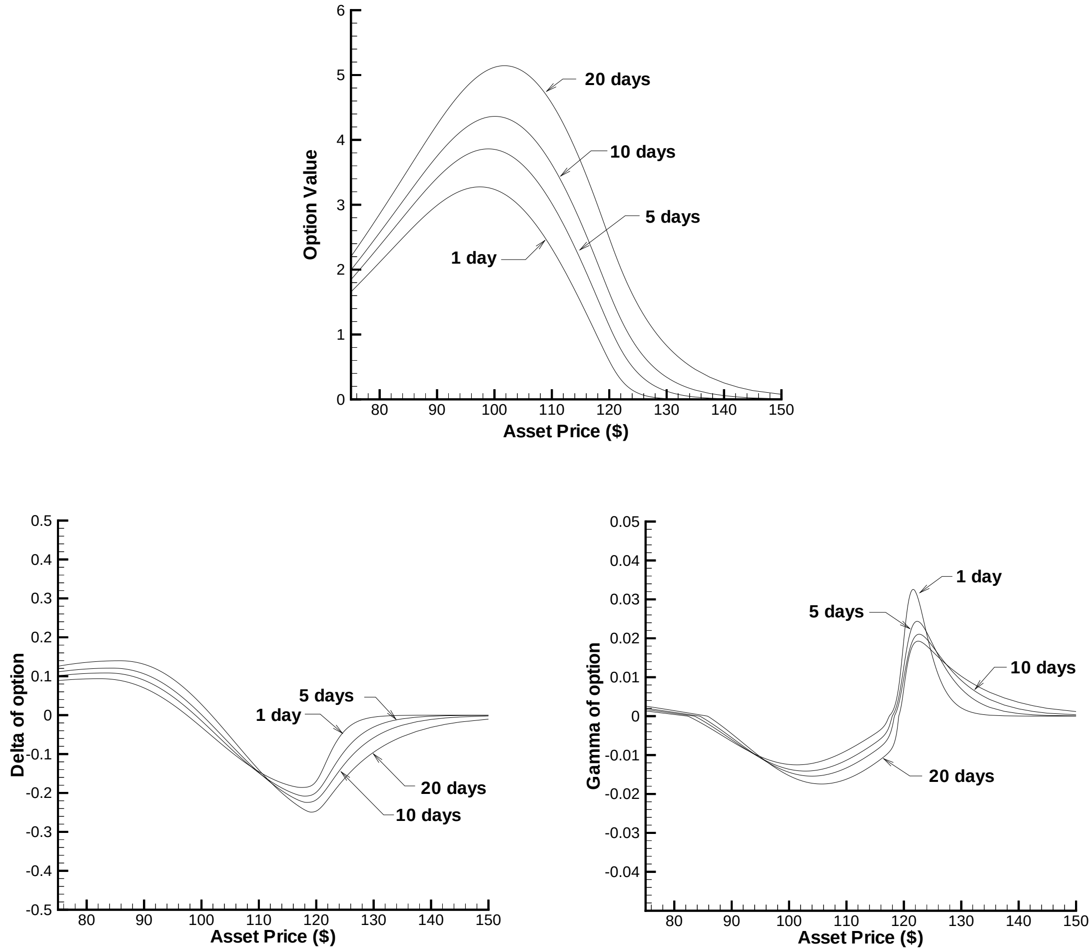

TABLE 4
Data for transaction cost model.

σ	.40
r	.05
Time to expiry	.5 years
Transaction cost parameter	$\alpha = .25$
Exercise price (K)	\$100
Barrier location	\$120
Barrier type	arithmetic step [17], observed daily
Time to full knockout	5, 10, 20 days

FIG. 5. *Worst case option value, delta (U_S) and gamma (U_{SS}). Step barrier (linear knockout, time to full knockout* $1, 5, 10, 20$ *days), barrier at \$120, barrier observed daily, call,* $T = .5$, $r = .05$, *range of* $\sigma = .25 - .50$.

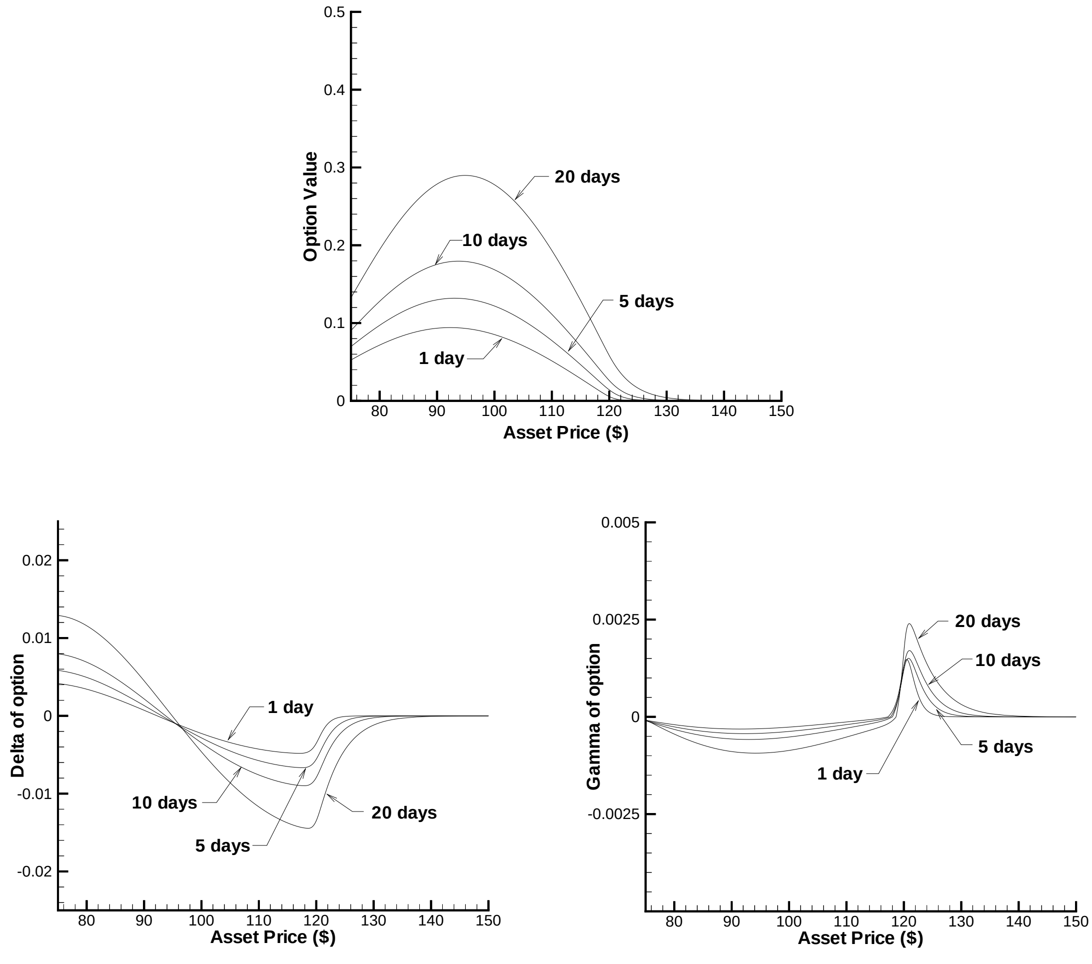

FIG. 6. *Option values with transaction costs. Step barrier (linear knockout, time to full knockout left: 5 days, middle: 10 days, right: 20 days.), barrier at \$120, barrier observed daily, call,* $T = .5$, $r = .05$, $\sigma = .40$, *transaction cost parameter* $\alpha = .25$.

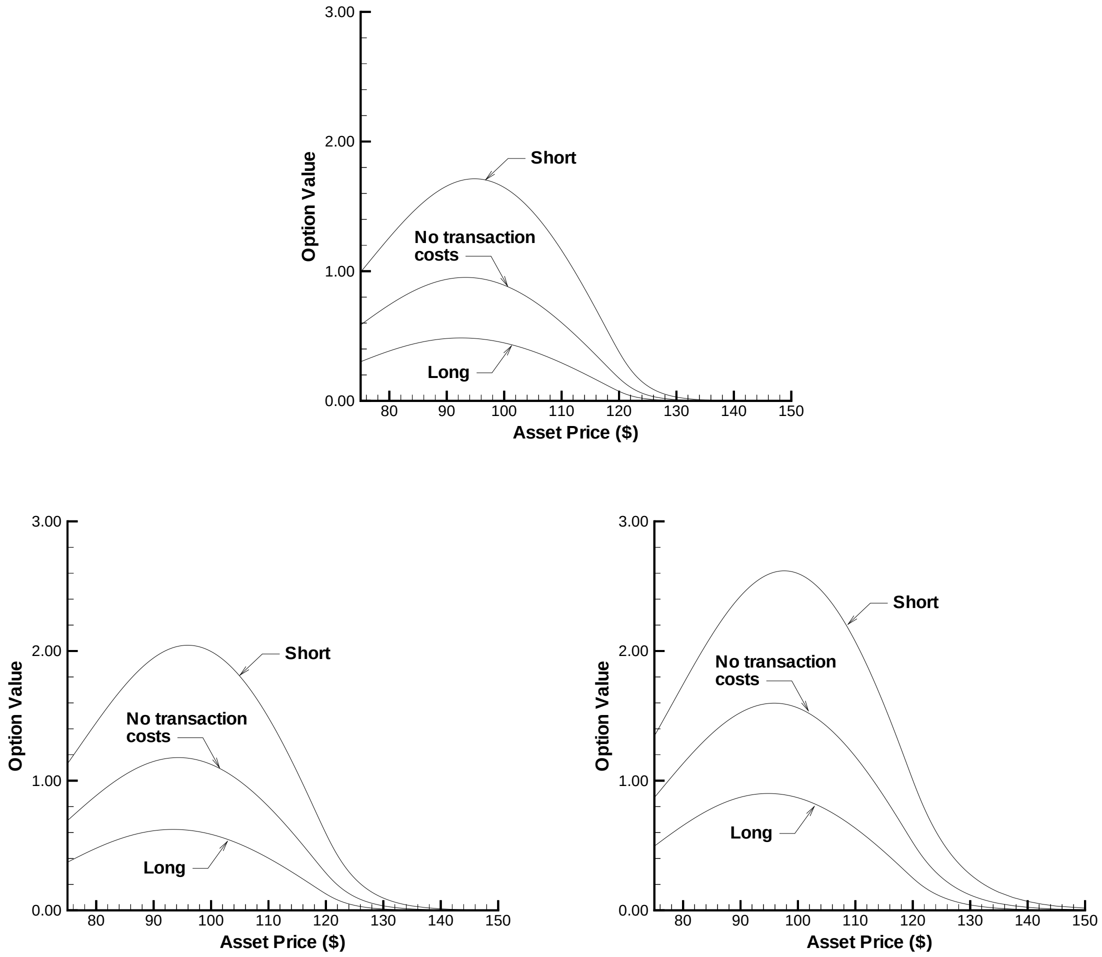

A straightforward application of Newton iteration to the nonlinear algebraic equations was superior to an approach which smoothed the discontinuity in the derivative near $\Gamma = U_{SS} = 0$. At $\Gamma = 0$, where the derivative is undefined, a limit from the left or right was used in the Jacobian. This did not appear to cause any convergence difficulties.

The uncertain volatility model had a very large effect on the spread in worst/best case prices (bid-ask prices) for a barrier option. A similar effect was observed for the spread between long-short prices for a transaction cost model. This was observed even though a linear arithmetic step barrier was specified, which should have the effect of reducing option gamma near the barrier, compared to an immediate knockout barrier.

REFERENCES

[1] L.B.G. Andersen and R. Brotherton-Ratcliffe. The equity option volatility smile: An implicit finite difference approach. *J. Comp. Fin.*, 1:5–37, Winter 1998.

[2] M. Avellaneda, A. Levy, and A Paras. Pricing and hedging derivative securities in markets with uncertain volatilities. *Appl. Math. Fin.*, 2:73–88, 1995.

[3] M. Avellaneda and A. Paras. Managing security risk of portfolios of derivative securities: The Lagrangian uncertain volatility model. *Appl. Math. Fin.*, 3:21–52, 1996.

[4] F. Black and M. Scholes. The pricing of options and corporate liabilities. *J. Pol. Econ.*, 81:637–59, 1973.

[5] P.P. Boyle and T. Vorst. Option replication in discrete time with transaction costs. *J. Fin.*, 47:271–293, 1992.

[6] L. Canina and S. Figlewski. The informational content of implied volatility. *Rev. Fin. Stud.*, 6:659–681, 1993.

[7] M. Chesney, J. Cornwall, M. Jeanblanc-Picqué, G. Kentwell, and M. Yor. Parisian pricing. *RISK*, 10:77–79, January 1997.

[8] M.H.A. Davis, V.G. Panas, and T. Zariphopoulou. European option pricing with transaction costs. *SIAM J. Cont. Opt.*, 31:470–493, 1993.

[9] B. Dumas, J. Fleming, and R.E. Whaley. Implied volatility functions: Empirical tests. *J. Fin.*, 53:2059–2106, 1998.

[10] S.D. Hodges and A. Neuberger. Optimal replication of contingent claims under transactions costs. *Rev. Fut. Markets*, 8:222–239, 1989.

[11] T. Hoggard, A.E. Whalley, and P. Wilmott. Hedging option portfolios in the presence of transaction costs. *Adv. Fut. Opt. Res.*, 7:21–35, 1994.

[12] J. Hull. *Options, Futures and Other Derivatives.* Prentice Hall, 1997.

[13] A. Jameson. Positive schemes and shock modelling for compressible flows. *Int. J. Num. Meth. Fluids*, 20:743–776, 1995.

[14] C. Johnson. *Numerical Solutions of Partial Differential Equations by the Finite Element Method.* Cambridge University Press, 1987.

[15] H.E. Leland. Option pricing and replication with transaction costs. *J. Fin.*, 40:1283–1301, 1985.

[16] V. Linetsky. Step options. *Math. Fin.*, forthcoming, 1998.

[17] V. Linetsky. Steps to the barrier. *RISK*, 11:62–65, April 1998.

[18] A.W. Lo and J. Wang. Implementing option pricing models when asset returns are predictable. *J. Fin.*, 50:87–127, 1995.

[19] R.C. Merton. Theory of rational option pricing. *Bell J. Econ. Man. Sci.*, 4:141–183, 1973.

[20] A. Paras and M. Avellaneda. Dynamic hedging with transaction costs: From lattice models to nonlinear volatility and free boundary problems. Preprint, Courant Institute of Mathematical Sciences, New York, 1995.

[21] M. Rubinstein. Implied binomial trees. *J. Fin.*, 49:771–818, 1994.

[22] K.R. Vetzal and P.A. Forsyth. Discrete Parisian and delayed barrier options: A general numerical approach. *Adv. Fut. Opt. Res.*, forthcoming, 1998.

[23] P. Wilmott. *Derivatives.* Wiley, 1998.

[24] M. Yor, M. Chesney, H. Geman, and M. Jeanblanc-Picqué. Some combinations of Asian, Parisian and barrier options. In M.A.H. Dempster and S.R. Pliska, editors, *Mathematics of Derivative Securities.* Cambridge University Press, 1997.

[25] R. Zvan, P.A. Forsyth, and K.R. Vetzal. A general finite element approach for PDE option pricing models. Working paper, Department of Computer Science, University of Waterloo, `http://yoho.uwaterloo.ca/~paforsyt/elem.ps`, 1998.

[26] R. Zvan, P.A. Forsyth, and K.R. Vetzal. A penalty method for American options with stochastic volatility. *J. Comp. Appl. Math.*, 91:199–218, 1998.

[27] R. Zvan, P.A. Forsyth, and K.R. Vetzal. Robust numerical methods for PDE models of Asian options. *J. Comp. Fin.*, 1:39–78, Winter 1998.

[28] R. Zvan, K.R. Vetzal, and P.A. Forsyth. Swing low, swing high. *RISK*, 11:71–75, March 1998.